Research Article

Petroleum and Chemical Industry International

Number of Moles Fractal Dimensions for Characterizing Shajara Reservoirs of the Shajara Formation, Saudi Arabia

Khalid Elyas Mohamed Elameen Alkhidir

Department of Petroleum and Natural Gas engineering, College of Engineering, King Saud University, Riyadh Saudi Arabia

***Corresponding author**
Khalid Elyas Mohamed Elameen Alkhidir, Department of Petroleum and Natural Gas engineering, College of Engineering, King Saud University, Riyadh Saudi Arabia, Tel: +966114679118; E-mail: kalkhidir@ksu.edu.sa

Submitted: 31 July 2018; **Accepted**: 06 Aug 2018; **Published**: 28 Aug 2018

Abstract

The quality and assessment of a reservoir can be documented in details by the application of number of moles. This research aims to calculate fractal dimension from the relationship among number of moles, maximum number of moles and wetting phase saturation and to confirm it by the fractal dimension derived from the relationship among capillary pressure and wetting phase saturation. In this research, porosity was measured on real collected sandstone samples and permeability was calculated theoretically from capillary pressure profile measured by mercury intrusion contaminating the pores of sandstone samples in consideration. Two equations for calculating the fractal dimensions have been employed. The first one describes the functional relationship between wetting phase saturation, number of moles, maximum number of moles and fractal dimension. The second equation implies to the wetting phase saturation as a function of capillary pressure and the fractal dimension. Two procedures for obtaining the fractal dimension have been utilized. The first procedure was done by plotting the logarithm of the ratio between number of mole and maximum number of moles versus logarithm wetting phase saturation. The slope of the first procedure = 3- Df (fractal dimension). The second procedure for obtaining the fractal dimension was concluded by plotting the logarithm of capillary pressure versus the logarithm of wetting phase saturation. The slope of the second procedure = Df -3. On the basis of the obtained results of the fabricated stratigraphic column and the attained values of the fractal dimension, the sandstones of the Shajara reservoirs of the Shajara Formation were divided here into three units. The gained units from bottom to top are: Lower Shajara number of moles Fractal Dimension Unit, Middle Shajara number of moles Fractal dimension Unit, and Upper Shajara number of moles Fractal Dimension Unit. The results show similarity between number of moles fractal dimension and capillary pressure fractal dimension. It was also noted that samples with wide range of pore radius were characterized by high values of fractal dimensions due to an increase in their connectivities which permit accommodation of high number of moles. In our case, and as conclusions the higher the fractal dimension, the higher the heterogeneity, the higher the permeability, the better the reservoir characteristics.

Keywords: Shajara Reservoirs, Shajara Formation, Number of moles fractal dimension

Introduction

The wetting phase saturation can be described as function of capillary pressure and fractal dimension was demonstrated byToledo GT et al [1]. The Purcell model was found to be the best fit to the experimental data of the wetting phase relative permeability for the cases as long as the measured capillary pressure curve had the same residual saturation as the relative permeability curve was described by Li K and Horne RN [2]. A theoretical model to correlate capillary pressure and resistivity index based on the fractal scaling theory was reported by Li K and Willams W [3]. The fractal dimension resulting from longer transverse NMR relaxation times and lower capillary pressure reflects the volume dimension of larger pores was described by Zhang Z and Weller A [4]. The fractal dimension derived from the short NMR relaxation times is similar to the fractal dimension of the internal surface was described by Zhang Z and Weller A [4]. The fractal dimensions can be used to represent the complexity degree and heterogeneity of pore structure, and the coexistence of dissolution pores and large intergranular pores of Donghetang sandstones contributes to a heterogeneous pore throat distribution and a high value of fractal dimension was reported byWang Z, et al. [5].The relationship among capillary pressure (PC), nuclear magnetic transverse relaxation time (T2) and resistivity index (I) was studied byGuo Y-h, et al. [6]. An increase of bubble pressure fractal dimension and pressure head fractal dimension and decreasing pore size distribution index and fitting parameters m*n due to possibility of having interconnected channels was confirmed byAlKhidir KEME [7]. An increase of fractal dimension with increasing arithmetic, geometric relaxation time of induced polarization, permeability and grain size was investigated by Alkhidir KEME [8,9,10]. An increase of seismo electric and resistivity fractal dimensions with increasing permeability and grain size was described byAlKhidir KEME [11,12].

Materials and Methods

Sandstone samples were collected from the surface type section of the Permo-Carboniferous Shajara Formation, latitude 2652 17.4, longitude 43 36 18. (Figure1). Porosity was measured on collected samples using mercury intrusion Porosimetry and permeability was derived from capillary pressure data. The purpose of this paper is to obtain number of moles fractal dimension and to confirm it by capillary pressure fractal dimension. The fractal dimension of the first procedure is determined from the positive slope of the plot of logarithm of the ratio of number of moles (NOM) to maximum number of moles (NOM_{max}) versus log wetting phase saturation (logSw). Whereas the fractal dimension of the second procedure is determined from the negative slope of the plot of logarithm of log capillary pressure (log (Pc) versus logarithm of wetting phase saturation (log Sw).

The number of moles can be scaled as

$$Sw = \left[\frac{NOM^{\frac{1}{2}}}{NOM_{max}^{\frac{1}{2}}}\right]^{[3-Df]} \quad 1$$

Where SW the water saturation, NOM the number of moles, Noma the maximum number of moles, and Df the fractal dimension.
Equation 1 can be proofed from

$$J = CEK * \Delta P \quad 2$$

Where J the electric current density in ampere / square meter, CEK the electro kinetic coefficient in ampere / (pascal*meter), and ΔP the pressure gradient in pascal /meter.
The electro kinetic coefficient can be scaled as

$$CEK = Cs * \sigma \quad 3$$

Where CEK the electro kinetic coefficient in ampere / (pascal * meter), Cs the streaming potential coefficient in volt / pascal, and σ the fluid electric conductivity in Siemens /meter.
Insert equation 3 into equation 2

$$J = Cs * \sigma * \Delta P \quad 4$$

The streaming potential coefficient can be scaled as

$$Cs = \left[\frac{\Psi}{\rho}\right] \quad 5$$

Where Cs the streaming potential coefficient in volt / pascal, Ψ the seismo electric transfer function in volt*square second /square meter, ρ the density in kilo gram / cubic meter.
Insert equation 5 into equation 4

$$J = \left[\frac{\Psi * \sigma * \Delta P}{\rho}\right] \quad 6$$

The density can be scaled as

$$\rho = \left[\frac{m}{V}\right] \quad 7$$

Where ρ the density in kilo gram /cubic meter, m the mass in kilo gram, and V the volume in cubic meter.
Insert equation 7 into equation 6

$$J * m = \Psi * \sigma * \Delta P * V \quad 8$$

The mass can be scaled as

$$m = NOM * mm \quad 9$$

Where m the mass in kilo gram, NOM the number of moles, and mm the molecular mass in kilo gram / mole.
Insert equation 9 into equation 8

$$J * NOM * mm = \Psi * \sigma \Delta P * V \quad 10$$

The electric conductivity can be scaled as

$$\sigma = \left[\frac{reff^2 * CE}{8 * \mu * Cs}\right] \quad 11$$

Where σ the electric conductivity of the fluid in Siemens /meter, reff the effective pore radius in meter, CE the electro osmosis coefficient in pascal / volt, µ the fluid viscosity in pascal * second, and Cs the streaming potential coefficient in volt / pascal.
Insert equation 11 into equation 10

$$J * NOM * mm = \left[\frac{\Psi * reff^2 * CE * \Delta P * V}{8 * \mu * Cs}\right] \quad 12$$

When the pore radius is introduced equation 12 will become

$$J * NOM * mm = \left[\frac{\Psi * r^2 * CE * \Delta P * V}{8 * \mu * Cs}\right] \quad 13$$

The maximum pore radius can be scaled as

$$J * NOM_{max} * mm = \left[\frac{\Psi * r_{max}{}^2 * CE * \Delta P * V}{8 * \mu * Cs}\right] \quad 14$$

Divide equation 13 by equation 14

$$\left[\frac{J * NOM * mm}{J * NOM_{max} * mm}\right] = \left[\frac{\left[\frac{\Psi * r^2 * CE * \Delta P * V}{8 * \mu * Cs}\right]}{\left[\frac{\Psi * r_{max}{}^2 * CE * \Delta P * V}{8 * \mu * Cs}\right]}\right] \quad 15$$

Equation 15 after simplification will become

$$\left[\frac{NOM}{NOM_{max}}\right] = \left[\frac{r^2}{r_{max}^2}\right] \quad 16$$

Take the square root of equation 16

$$\sqrt{\left[\frac{NOM}{NOM_{max}}\right]} = \sqrt{\left[\frac{r^2}{r_{max}^2}\right]} \quad 17$$

Equation 17 after simplification will become

$$\left[\frac{NOM^{\frac{1}{2}}}{NOM_{max}^{\frac{1}{2}}}\right] = \left[\frac{r}{r_{max}}\right] \quad 18$$

Take the logarithm of equation 18

$$\log\left[\frac{NOM^{\frac{1}{2}}}{NOM_{max}^{\frac{1}{2}}}\right] = \log\left[\frac{r}{r_{max}}\right] \quad 19$$

$$\text{But; } \log\left[\frac{r}{r_{max}}\right] = \frac{\log Sw}{[3 - Df]} \quad 20$$

Insert equation 20 into equation 19

$$\frac{\log Sw}{[3 - Df]} = \log\left[\frac{NOM^{\frac{1}{2}}}{NOM_{max}^{\frac{1}{2}}}\right] \quad 21$$

Equation 21 after log removal will become

$$Sw = \left[\frac{NOM^{\frac{1}{2}}}{NOM_{max}^{\frac{1}{2}}}\right]^{[3-Df]} \quad 22$$

Equation 22 the proof of equation 1 which relates the water saturation, the number of moles, the maximum number of moles, and the fractal dimension.

The capillary pressure can be scaled as

log Sw = [Df - 3] * log pc + constant **23**

Where Sw the water saturation, DF the fractal dimension, and pc the capillary pressure.

Result and discussion

Based on field observation the Shajara Reservoirs of the Permo-Carboniferous Shajara Formation were divided here into three units as described in Figure1.These units from bottom to top are: Lower Shajara Reservoir, Middle Shajara reservoir, and Upper Shajara Reservoir. Their acquired results of the number of moles fractal dimension and capillary pressure fractal dimension are displayed in Table 1. Based on the attained results it was found that the number of moles fractal dimension is equal to the capillary pressure fractal dimension. The maximum value of the fractal dimension was found to be 2.7872 assigned to sample SJ13 from the Upper Shajara Reservoir as verified in Table 1. Whereas the minimum value of the fractal dimension 2.4379 was reported from sample SJ3 from the Lower Shajara reservoir as displayed in Table1. The number of moles fractal dimension and capillary pressure fractal dimension were observed to increase with increasing permeability as proofed in Table1 owing to the possibility of having interconnected channels.

The Lower Shajara reservoir was denoted by six sandstone samples (Figure 1), four of which label as SJ1, SJ2, SJ3 and SJ4 were selected for capillary pressure measurement as confirmed in Table1. Their positive slopes of the first procedure log of the ratio of number of moles (NOM) to maximum number of moles (NOM_{max}) versus log wetting phase saturation (Sw) and negative slopes of the second procedure log capillary pressure (Pc) versus log wetting phase saturation (Sw) are delineated in Figure 2, Figure 3, Figure 4, and Figure 5. Their number of moles fractal dimension and capillary pressure fractal dimension values are shown in Table 1. As we proceed from sample SJ2 to SJ3 a pronounced reduction in permeability due to compaction was reported from 1955 md to 56 md which reflects decrease in number of moles fractal dimension from 2.7748 to 2.4379 as specified in table 1. Again, an increase in grain size and permeability was verified from sample SJ4 whose number of moles fractal dimension and capillary pressure fractal dimension was found to be 2.6843 as described in Table 1.

Formation	Reservoir	Sample	Porosity %	k (md)	Positive slope of the first procedure Slope=3-Df	Negative slope of the second procedure Slope=Df-3	Number of moles fractal dimension	Capillary pressure fractal dimension
Permo-Carboniferous Shajara Formation	Upper Shajara Reservoir	SJ13	25	973	0.2128	-0.2128	2.7872	2.7872
		SJ12	28	1440	0.2141	-0.2141	2.7859	2.7859
		SJ11	36	1197	0.2414	-0.2414	2.7586	2.7586
	Middle Shajara Reservoir	SJ9	31	1394	0.2214	-0.2214	2.7786	2.7786
		SJ8	32	1344	0.2248	-0.2248	2.7752	2.7752
		SJ7	35	1472	0.2317	-0.2317	2.7683	2.7683
	Lower Shajara Reservoir	SJ4	30	176	0.3157	-0.3157	2.6843	2.6843
		SJ3	34	56	0.5621	-0.5621	2.4379	2.4379
		SJ2	35	1955	0.2252	-0.2252	2.7748	2.7748
		SJ1	29	1680	0.2141	-0.2141	2.7859	2.7859

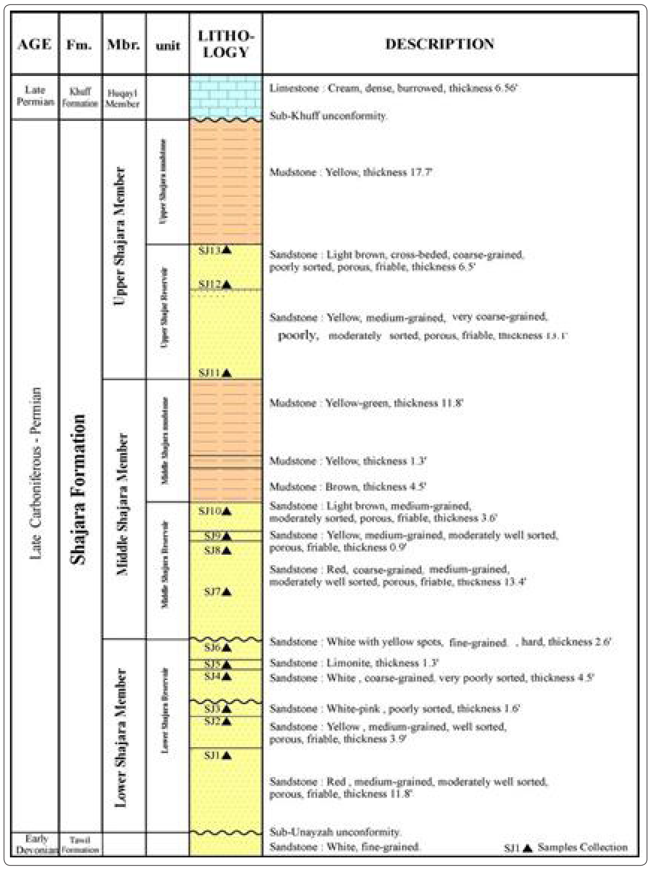

Figure 1: Surface type section of the Shajara Reservoirs of the Permo-Carboniferous Shajara formation at latitude 26 52 17.4, longitude 43 36 18.

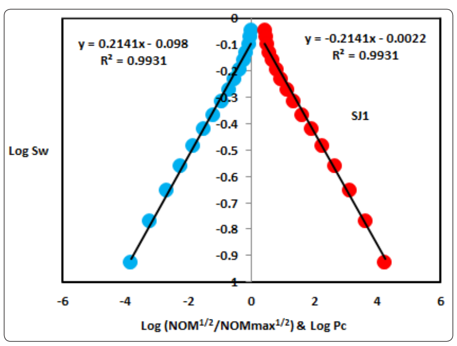

Figure 2: Log ($NOM^{1/2}$ /$NOM^{1/2}_{max}$) & log Pc versus log Sw of sample SJ1

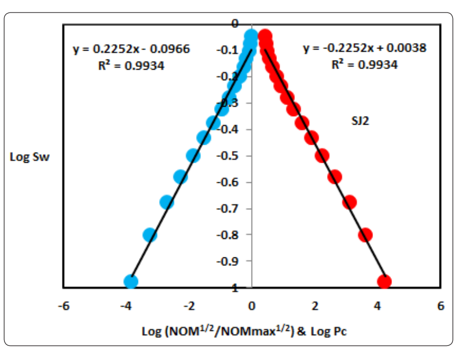

Figure 3: Log ($NOM_{1/2}$ /$NOM^{1/2}_{max}$) & log Pc versus log Sw of sample SJ2

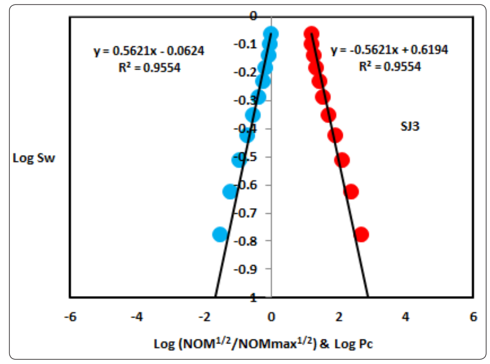

Figure 4: Log ($NOM^{1/2}$ /$NOM^{1/2}_{max}$) & log Pc versus log Sw of sample SJ3

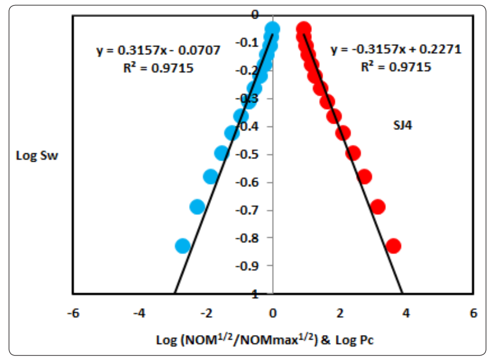

Figure 5: Log ($NOM^{1/2}$ /$NOM^{1/2}_{max}$) & log Pc versus log Sw of sample SJ4

In contrast, the Middle Shajara reservoir which is separated from the Lower Shajara reservoir by an unconformity surface as shown in Figure 1. It was designated by four samples (Figure 1), three of which named as SJ7, SJ8, and SJ9 as illustrated in Table1 were selected for capillary measurements as described in Table 1. Their positive slopes of the first procedure and negative slopes of the second procedure are shown in Figure 6, Figure 7 and Figure 8 and Table 1. Additionally, their number of moles fractal dimensions and capillary pressure fractal dimensions show similarities as delineated in Table 1.Their fractal dimensions are higher than those of samples SJ3 and SJ4 from the Lower Shajara Reservoir due to an increase in their permeability as explained in Table 1. On the other hand, the Upper Shajara reservoir was separated from the Middle Shajara reservoir by yellow green mudstone as revealed in Figure 1. It is defined by three samples so called SJ11, SJ12, SJ13 as explained in Table 1. Their positive slopes of the first procedure and negative slopes of the second procedure are displayed in Figure 9, Figure 10 and Figure 11 and Table 1. Moreover, their number of moles fractal dimension and capillary pressure fractal dimension are also higher thanthose of sample SJ3 and SJ4 from the Lower Shajara Reservoir due to an increase in their permeability as clarified in Table 1.

Overall a plot of number of moles fractal dimension versus capillary pressure fractal dimension as shown in Figure 12 reveals three permeable zones of varying Petrophysical properties. Such variation in fractal dimension can account for heterogeneity which is a key parameter in reservoir quality assessment. This reservoir heterogeneity was also confirmed by plotting positive slope of the first procedure versus negative slope of the second procedure as described in Figure 13.

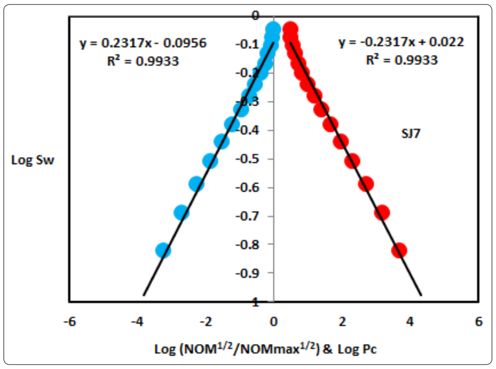

Figure 6: Log ($NOM^{1/2}$ /$NOM^{1/2}_{max}$) & log Pc versus log Sw of sample SJ7

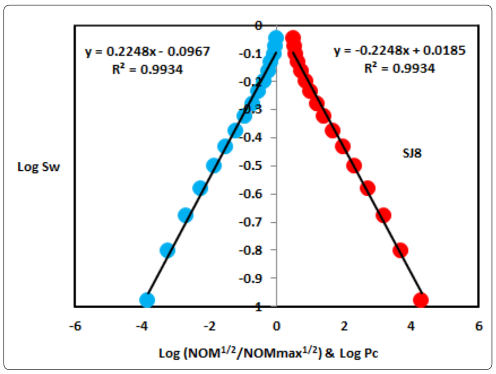

Figure 7: Log ($NOM^{1/2}$ /$NOM^{1/2}_{max}$) & log Pc versus log Sw of sample SJ8

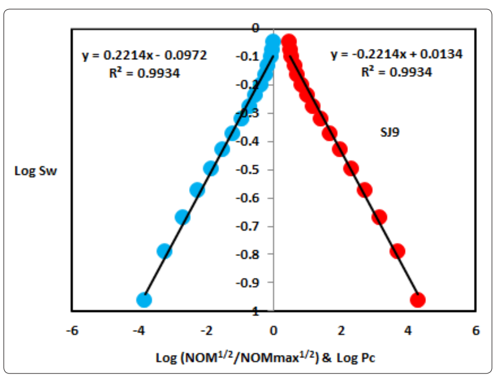

Figure 8: Log ($NOM^{1/2}$ /$NOM^{1/2}_{max}$) & log Pc versus log Sw of sample SJ9

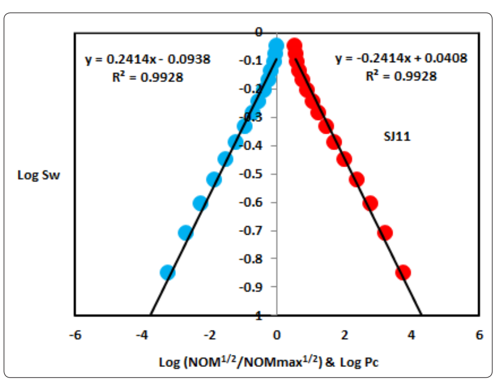

Figure 9: Log ($NOM^{1/2}$ /$NOM^{1/2}_{max}$) & log Pc versus log Sw of sample SJ11

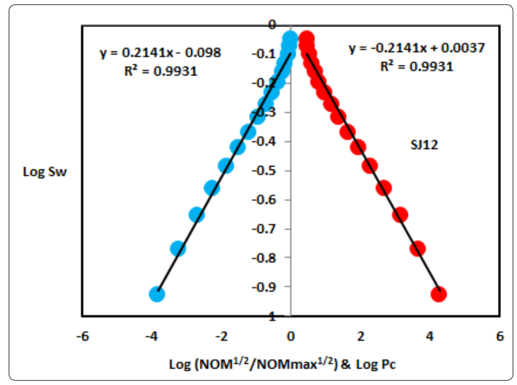

Figure 10: Log ($NOM^{1/2}$ /$NOM^{1/2}_{max}$) & log Pc versus log Sw of sample SJ12

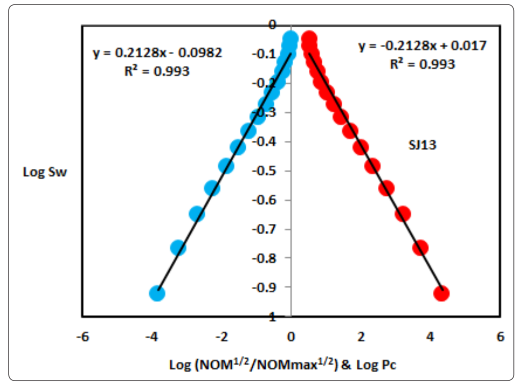

Figure 11: Log ($NOM^{1/2}$ /$NOM^{1/2}_{max}$) & log Pc versus log Sw of sample SJ13

Overall a plot of number of moles fractal dimension versus capillary pressure fractal dimension as shown in Figure 12 reveals three permeable zones of varying Petrophysical properties. Such variation in fractal dimension can account for heterogeneity which is a key parameter in reservoir quality assessment. This reservoir heterogeneity was also confirmed by plotting positive slope of the first procedure versus negative slope of the second procedure as described in Figure 13.

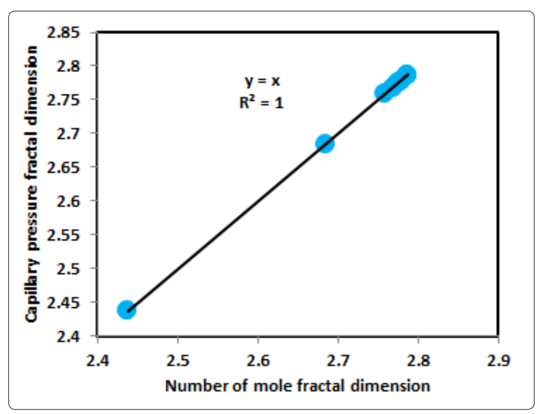

Figure 12: Number of moles fractal dimension versus capillary pressure fractal dimension

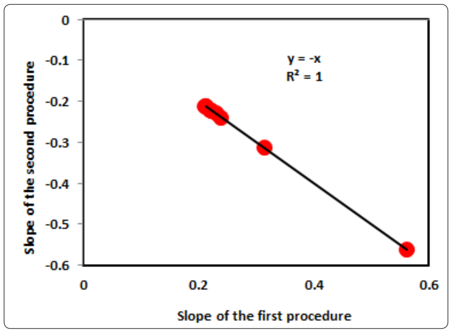

Figure 13: Slope of the first procedure versus slope of the second procedure

Conclusion

- The sandstones of the Shajara Reservoirs of the Shajara formation permo-Carboniferous were divided here into three units based on number of moles fractal dimension
- The Units from base to top are: Lower Shajara number of molesFractal dimension Unit, Middle Shajara number of molesFractal Dimension Unit, and Upper Shajara number of molesFractal Dimension Unit.
- These units were also proved by capillary pressure fractal dimension.
- The fractal dimension was found to increase with increasing grain size and permeability

Acknowledgement

The author would to thank King Saud University, College of Engineering, Department of Petroleum and Natural Gas Engineering, Department of Chemical Engineering, Research Centre at College of Engineering, and King Abdullah Institute for Research and Consulting Studies for their Supports.

References

1. Toledo GT, Navy RA, Davis HT, Scriven LE (1994) Capillary pressure, water relative permeability, electrical conductivity and capillary dispersion coefficient of fractal porous media at low wetting phase saturation. SPE advanced technology Series 2: 136-141.
2. Li K, Horne RN (2002) Experimental verification of methods to calculate relative permeability using capillary pressure data. SPE 76757, Proceedings of the 2002 SPE Western Region Meeting/ AAPG Pacific Section Joint Meeting held in Anchorage, Alaska.
3. Li K, Willams W (2007) Determination of capillary Pressure function from resistivity data. Transp. Porous Media 67: 1-15.
4. Zhang Z, Weller A (2014) Fractal Dimension of Pore-Space Geometry of Eocene sandstone formation. Geophysics 79: D377-D387.
5. Wang Z, Pan M, Shi Y, Liu L, Xiong F, et al. (2018) Fractal analysis of Donghetangs and stones using NMR measurements. Energy & Fuels 32: 2973-2982.
6. Guo Y-h, Pan B-z, Zhang L-h, Fang C-h (2018) Research and application of the relationship between transverse relaxation time and resistivity index in tight sandstone reservoir. J Petrol Sci Eng 160: 597-604.
7. AlKhidir KEME (2017) Pressure head fractal dimension for characterizing Shajara Reservoirs of the Shajara Formation of the Permo-Carboniferous Unayzah Group, Saudi Arabia. Arch Pet Environ Biotechnol 1-7.
8. Alkhidir KEME (2018) Arithmetic relaxation time of induced polarization fractal dimension for characterizing Shajara Reservoirs of the Shajara Formation. Nanosci Nanotechnol 2: 1-8.
9. Alkhidir KEME (2018) Geometric relaxation time of induced polarization fractal dimensionfor characterizing Shajara Reservoirs of the Shajara formation of the Permo-Carboniferous Unayzah Group-Permo. Int J Pet Res 2: 105-108.
10. Alkhidir KEME (2018) Geometric relaxation time of induced polarization fractal dimensionfor characterizing Shajara Reservoirs of the Shajara Formation of the Permo-Carboniferous Unayzah Group, Saudi Arabia. SF J Petroleum 2: 1-6.
11. AlKhidir KEME (2018) Seismo electric field fractal dimension for characterizing Shajara Reservoirs of the Permo-Carboniferous Shajara Formation, Saudi Arabia. Pet Petro Chem Eng J 2: 1-8.
12. Alkhidir KEME (2018) Resistivity fractal dimension for characterizing Shajara Reservoirs of the Permo Carboniferous Shajara Formation Saudi Arabia. Recent Adv. Petrochem Sci 5: 1-6.